7-1-2015

Role of Phenol-Soluble Modulins in Formation of Staphylococcus aureus Biofilms in Synovial Fluid.

Sana S Dastgheyb
Pathogen Molecular Genetics Section, Laboratory of Human Bacterial Pathogenesis, National Institute of Allergy and Infectious Diseases, National Institutes of Health; Department of Orthopedic Surgery, Thomas Jefferson University

Amer E Villaruz
Pathogen Molecular Genetics Section, Laboratory of Human Bacterial Pathogenesis, National Institute of Allergy and Infectious Diseases, National Institutes of Health

Katherine Y Le
Pathogen Molecular Genetics Section, Laboratory of Human Bacterial Pathogenesis, National Institute of Allergy and Infectious Diseases, National Institutes of Health

Vee Y Tan
Pathogen Molecular Genetics Section, Laboratory of Human Bacterial Pathogenesis, National Institute of Allergy and Infectious Diseases, National Institutes of Health

Anthony C Duong
Pathogen Molecular Genetics Section, Laboratory of Human Bacterial Pathogenesis, National Institute of Allergy and Infectious Diseases, National Institutes of Health

Authors
Sana S Dastgheyb, Amer E Villaruz, Katherine Y Le, Vee Y Tan, Anthony C Duong, Som S Chatterjee, Gordon Y C Cheung, Hwang-Soo Joo, Noreen J Hickok, and Michael Otto

IAI Journals.ASM.org

Role of Phenol-Soluble Modulins in Formation of *Staphylococcus aureus* Biofilms in Synovial Fluid

Sana S. Dastgheyb,[a,b] Amer E. Villaruz,[a] Katherine Y. Le,[a] Vee Y. Tan,[a] Anthony C. Duong,[a] Som S. Chatterjee,[a]* Gordon Y. C. Cheung,[a] Hwang-Soo Joo,[a] Noreen J. Hickok,[b] Michael Otto[a]

Pathogen Molecular Genetics Section, Laboratory of Human Bacterial Pathogenesis, National Institute of Allergy and Infectious Diseases, National Institutes of Health, Bethesda, Maryland, USA[a]; Department of Orthopedic Surgery, Thomas Jefferson University, Philadelphia, Pennsylvania, USA[b]

***Staphylococcus aureus* is a leading cause of prosthetic joint infections, which, as we recently showed, proceed with the involvement of biofilm-like clusters that cause recalcitrance to antibiotic treatment. Here we analyzed why these clusters grow extraordinarily large, reaching macroscopically visible extensions (>1 mm). We found that while specific *S. aureus* surface proteins are a prerequisite for agglomeration in synovial fluid, low activity of the Agr regulatory system and subsequent low production of the phenol-soluble modulin (PSM) surfactant peptides cause agglomerates to grow to exceptional dimensions. Our results indicate that PSMs function by disrupting interactions of biofilm matrix molecules, such as the polysaccharide intercellular adhesin (PIA), with the bacterial cell surface. Together, our findings support a two-step model of staphylococcal prosthetic joint infection: As we previously reported, interaction of *S. aureus* surface proteins with host matrix proteins such as fibrin initiates agglomeration; our present results show that, thereafter, the bacterial agglomerates grow to extremely large sizes owing to the lack of PSM expression under the specific conditions present in joints. Our findings provide a mechanistic explanation for the reported extreme resistance of joint infection to antibiotic treatment, lend support to the notions that Agr functionality and PSM production play a major role in defining different forms of *S. aureus* infection, and have important implications for antistaphylococcal therapeutic strategies.**

Staphylococcus aureus is a major cause of septic arthritis and orthopedic infections, in particular those developing on prosthetic joints after arthroplasty (1). In the presence of a prosthetic device, joint infection rates are at about 1 to 2% (2). Joint infections can cause prolonged disability and increased health care costs, due to prolonged antibiotic treatment, multiple surgeries, and, in difficult cases, joint fusion. If recalcitrant to treatment, these infections can cause significant morbidity, including loss of limb, systemic infection, and even death (3).

Antibiotic treatment alone is usually insufficient to eradicate joint infections. We recently showed that the pronounced recalcitrance of *S. aureus* joint infections to antibiotic treatment is due to exceptionally strong bacterial aggregation and biofilm formation, which renders even the high concentrations of antibiotics given prophylactically to patients ineffective (4). Biofilms are surface-attached bacterial agglomerations that frequently develop on indwelling medical devices (5). The matrix that connects cells in a biofilm consists of a variety of chemically different macromolecules, such as polymeric proteins, teichoic acids, extracellular DNA (eDNA), and polysaccharides (6). The polysaccharide intercellular adhesin (PIA; also named poly-*N*-acetylglucosamine [PNAG]) is the main biofilm exopolysaccharide in staphylococci (7, 8).

Using a genome-wide screen, our previous work identified specific *S. aureus* factors that are crucial for the establishment of biofilms and biofilm-like aggregates in synovial fluid (SF) isolated from traumatized joints (4). These included, first and foremost, surface-attached proteins that bind to human fibrin and fibronectin, which are human matrix proteins that are present in traumatized and infected joints (1, 9). *S. aureus* mutants defective in the fibrinogen-binding protein ClfA or ClfB, or the fibronectin-binding protein FnbA or FnbB, were unable to produce the macroscopic aggregates that the corresponding wild-type strain formed in SF.

In the present study, we analyzed the mechanistic underpinnings of the exceptionally high level of aggregate formation in SF, by testing whether this extreme phenotype is due to altered expression of distinct bacterial factors. In addition to evaluating whether altered expression of the aforementioned surface binding proteins plays a role, we analyzed whether the accessory gene regulator (Agr) and the Agr-regulated phenol-soluble modulins (PSMs) are involved. The accessory gene regulator (Agr) is a quorum-sensing system in charge of regulating virulence traits in staphylococci depending on the density of the bacterial population (10). Notably, it is a master regulator of biofilm formation (11, 12). *In vitro*, *agr* deletion mutants of *S. aureus* and *S. epidermidis* grow thicker and less structured biofilms than the isogenic wild-type strains (13–15).

PSMs are main molecular effectors of the impact that Agr has on biofilm development (13, 15). They are under strict and direct

Received 23 March 2015 **Returned for modification** 16 April 2015
Accepted 2 May 2015

Accepted manuscript posted online 11 May 2015

Citation Dastgheyb SS, Villaruz AE, Le KY, Tan VY, Duong AC, Chatterjee SS, Cheung GYC, Joo H-S, Hickok NJ, Otto M. 2015. Role of phenol-soluble modulins in formation of *Staphylococcus aureus* biofilms in synovial fluid. Infect Immun 83:2966–2975. doi:10.1128/IAI.00394-15.

Editor: A. Camilli

Address correspondence to Michael Otto, motto@niaid.nih.gov.

* Present address: Som S. Chatterjee, San Francisco General Hospital, University of California San Francisco, San Francisco, California, USA.

doi:10.1128/IAI.00394-15

control of Agr by direct binding of the AgrA response regulator to the *psm* operon promoters (16). There are three loci in *S. aureus* that encode PSMs: the *psm*α locus encodes the peptides PSMα1 through PSMα4; the *psm*β locus encodes PSMβ1 and PSMβ2; and RNAIII includes the gene encoding the PSM δ-toxin (17, 18). *In vitro* studies using TSB growth medium showed that all *S. aureus* PSMs impact biofilm formation in a similar way (13), i.e., they structure biofilms and lead to biofilm dispersal, which is likely due to their surfactant properties. While PSMs are important for biofilm structuring and thus biofilm development, the overall impact of PSMs on the extent of biofilm formation is negative because PSMs disperse biofilms (13, 15). Thus, these factors could not be identified in our recent work, which sought to identify factors with a generally positive impact on biofilm-like aggregation (4). Notably, the role of PSMs during *S. aureus in vivo* biofilm infection is not well understood. While the PSM-mediated dispersal effect has been shown to promote systemic dissemination of biofilm-associated infection, it is not known if lack of PSM production also leads to more extensive *in vivo* biofilm formation on indwelling devices (13).

In the present study, we show that low activity of Agr and low PSM production in SF are a major cause for the exceptionally strong aggregation behavior of *S. aureus* in SF. We demonstrate that PSM production has a key role in defining biofilm extension under conditions that exemplify an *in vivo* situation and provide evidence that contributes to our understanding of how PSMs affect biofilm dispersal.

MATERIALS AND METHODS

Ethics statement. Human SF was drained from the joint during total knee arthroplasty in the operating room and collected with permission of the Thomas Jefferson University Institutional Review Board (IRB). A waiver for the requirement of informed written consent was obtained, because the samples were deidentified, obtained during routine procedures, and would normally have been discarded. Human serum was obtained from the blood bank of the NIH with an existing IRB protocol.

Preparation and storage of SF. SF that was obtained as mentioned above was stored at 4°C for a period not exceeding 6 months before use. Cellularity was not recorded. All samples containing blood upon visual examination were discarded. Of note, due to the conditions of storage, white blood cells were inactive (dead) at the time of use of SF for our experiments.

Strains and growth conditions. All experiments were performed using strain *S. aureus* LAC (pulsed-field type USA300), a community-associated methicillin-resistant strain, or its derivatives. The USA300 lineage is the main source of skin and prosthetic-joint infections (PJIs) in the United States (19, 20). The total Δ*psm* mutant (with the *psm*α and *psm*β operons deleted and translation of δ-toxin abolished by mutation of the *hld* gene start codon) and the Δ*agr* mutant of LAC were produced by sequential allelic replacement and by phage transduction from strain RN6911, respectively, and were previously described (18, 21). Of note, the LAC wild-type strain and its Δ*agr* and Δ*psm* mutants do not show significant differences in growth rates and yield in SF when grown at 37°C in shaking incubators (data not shown). Strain LAC was transformed by electroporation with plasmids based on the pTX_{Δ} plasmid background, constitutively expressing the *psm*α (15), *psm*β (this study), *hld* (22), or *agrA* (16) gene/operon under the control of the *xyl* promoter. The *xyl* repressor gene has been removed in that plasmid series to produce a constitutive mode of expression (18). The control strain harbors the corresponding $pTX_{\Delta}16$ plasmid (18). Strains were grown in SF, serum, or tryptic soy broth (TSB), as indicated. Oligonucleotides used are shown in Table 1, and strains used are shown in Table 2.

Macroscopic determination of bacterial aggregation. Aggregate formation was monitored by UV-fluorescent imaging of ethidium bromide (EtBr)-labeled bacteria (10 μg/ml EtBr, 10 min in the dark).

Measurement of aggregate size distribution. Aggregate size distribution was measured using a T3 Cellometer (Nexcelom) as described previously (4). Briefly, overnight cultures were centrifuged and resuspended to a concentration of ~10^{10} CFU/ml in sterile phosphate-buffered saline (PBS). One milliliter of SF, TSB, or serum was prewarmed to 37°C, 5 μl of the bacterial suspension and 20 μl of trypan blue were added, and the sample was incubated for 20 min at 37°C with agitation. The Cellometer can detect aggregates between 3 and 100 μm in size. The parameters were set to detect oddly shaped aggregates (roundness was not set as a determining factor).

qRT-PCR. Strain LAC (initial inoculum 10^4 CFU/ml) was grown for 8 h in TSB, SF, or serum, in a shaking incubator at 180 rpm and 37°C. mRNA was collected using the RNeasy minikit (Qiagen), and quantitative real-time PCR (qRT-PCR) was performed as described previously (23). Oligonucleotides used are described in Table 1. All probes were labeled with 5′-carboxyfluorescein. All experiments were performed in triplicate, and data were normalized against the housekeeping *gyrB* gene.

Creation of luciferase reporter gene fusion constructs and luminescence measurement. The *lux* operon (*luxABCDE*; 5.7 kb) was amplified from plasmid pXen5 (kindly given by K. Francis) (24) using the primers *lux*BamHI and *lux*SalI and cloned into plasmid pLL29 (a gift from C. Lee) (25). The P2, P3, *psm*α, and *psm*β promoters were amplified from LAC genomic DNA and cloned into the resulting plasmid, pLL29*lux*, using SacI/BamHI (*psm*β promoter) or EcoRI/BamHI (all other promoters) restriction sites. Then, the integration procedure protocol was performed as described previously (25). Briefly, the pLL29*lux* reporter fusion plasmids were electroporated into strain RN4220 carrying plasmid pLL2787, which contains the ϕ11 *int* gene. After selecting for clones in which the integration of the respective pLL29 plasmid into the host *attB* sites had occurred, the chromosome-integrated pLL29 plasmids carrying the respective *lux* reporter fusion were phage transduced into strain LAC. Correct integration was verified by analytical PCR. Light emitted by the luciferase gene reporter fusion constructs was measured using a Victor (Perkin-Elmer) instrument.

Immunoblotting test for PIA. Strain LAC was inoculated at 10^4 CFU from a preculture grown in TSB and grown for 24 h at 37°C and 180 rpm in 1 ml of either TSB, serum, or SF. Immunodetection of polysaccharide intercellular adhesin (PIA) was then performed as described by Cramton et al. (26) to minimize cross-reactivity to protein A. In brief, all cultures were resuspended in 1 ml TSB to an optical density at 600 nm (OD_{600}) of 10.0. Each sample was centrifuged and resuspended in 0.5 M EDTA (pH 8.0) and incubated for 5 min at 100°C. Samples were centrifuged and 40 μl of supernatant were incubated with 10 μl proteinase K (20 mg/ml) for 30 min at 37°C. A 3.5-μl portion of each sample was spotted onto nitrocellulose, dried, and blocked with 3% bovine serum albumin (BSA) for 1 h prior to the addition of anti-PIA serum (1:1,000; from rabbit). The membrane was then incubated at 4°C for 18 h. Afterwards, it was washed five times with Tris-buffered saline (TBS)–Tween (0.1%) and incubated for 2 h with Cy5-labeled goat anti-rabbit IgG (Life Technologies), followed by washing five times with TBS-Tween (0.1%). Signals were detected using a Typhoon Trio variable-mode imager (GE Healthcare).

SEM. To prepare for scanning electron microscopy (SEM), samples were fixed with 2% paraformaldehyde in 0.1 M sodium phosphate buffer. Samples were then sent to the SEM facility at Rocky Mountain Laboratories, NIAID, where they were sputter coated using a South Bay Technology IBS/e instrument and imaged on a Hitachi SU8000 electron microscope.

Biofilm assays. For biofilm analysis by confocal laser scanning microscopy (CLSM), strains were incubated in TSB under static conditions in an 8-well borosilicate plate for 8 h. TSB was aspirated, replaced with 200 μl of SF, and incubated for a further 24 h. Samples were then washed gently three times with sterile PBS, stained with 4 μM propidium iodide for 30

TABLE 1 Oligonucleotides used in this study

Use and primer	Sequence
qRT-PCR	
RNAIII-for	GTGATGGAAAATAGTTGATGAGTTGTTT
RNAIII-rev	GAATTTGTTCACTGTGTCGATAATCC
RNAIII probe	TGCACAAGATATCATTTCAACAATCAGTGACTTAGTAAAA
psmα-for	TATCAAAAGCTTAATCGAACAATTC
psmα-rev	CCCCTTCAAATAAGATGTTCATATC
psmα probe	AAAGACCTCCTTTGTTTGTTATGAAATCTTATTTACCAG
agrA-for	CGTAAGCATGACCCAGTTGGT
agrA-rev	CCATCGCTGCAACTTTGTAGAC
agrA probe	ATTATTTTCGTTACGAGTCACAGTGAACT
icaA-for	TGAACCGCTTGCCATGTG
icaA-rev	CACGCGTTGCTTCCAAAGA
icaA probe	TGGATGTTGGTTCCAGAAACATTGGGAG
clfA-for	AGGTTCTGGTGACGGTATCGA
clfA-rev	TCAATTTCACCAGGCTCATCAG
clfA probe	AAACCAGTTGTTCCTGAAC
clfB-for	TTCCAATGCGCAAGGAACTAG
clfB-rev	CAGCATTTACTACAGGTTCAGCAACT
clfB probe	AGACTACGTACAGCTCTCGTTCTAACACTT
fnbA-for	TGAGCCAGAAACTCCAACAC
fnbA-rev	TGGCAGGTGGTACTGGTTTA
fnbA probe	CGCCAACACCAGAGGTACCAGC
fnbB-for	AGGAATTAAGGCGGGAGATT
fnbB-rev	TGTCGCCATAACTTGACCAT
fnbB probe	CTCAACACTGCGTAAAGTTCCGGAGA
rsbU-for	ACCATAACGATGGCACAATG
rsbU -rev	TCCATAAGAATCCATGCCAA
rsbU probe	TCCCAATGACATCTGCAACAGCA
TRAP-for	CGTTTGTTAAGACCTGCTAAAGG
TRAP-rev	TGTCCGCTTGAACCAAAGTA
TRAP probe	TGCATGTCGATCAGCAAATCCG
Luciferase reporter gene fusion construction and verification	
luxBamHI	ATGCGGATCCTGCAGATGAAGCAAGAGGAG
luxSalI	ATGCGTCGACGCAGCGGTATTTTTCGATCA
P2prEco	ATGCGAATTCCTCATCAACTATTTTCCATCACATCTCTGT
P2prBam	CAATTTTACACCACTCTCCTCACTGGGATCCCATTATACG
P3prBam	ATGCGGATCCCTCATCAACTATTTTCCATCACATCTCTGT
P3prEco	CAATTTTACACCACTCTCCTCACTGGAATTCCATTATACG
psmβprSacI	GGCTTAGAAGGCCATTGCTGAGCTCAGCTGAGCTACCAGG
psmβprBam	TATCTTTAATTGCGTTAAATAAACCTTCCATTGAAAACAGGATCCAAAA
psmαprEco	GCCTAGACGAGACCTAACGTGGAATTCGTTTTAAAC
psmαprBam	GATGCCAGCGATGATACCCATTAAGATTGGATCCTTGCTTAT
scv4	ACCCAGTTTGTAATTCCAGGAG
scv8	GCACATAATTGCTCACAGCCA
scv9	GCTGATCTAACAATCCAATCCA
scv10	TATACCTCGATGATGTGCATAC
Cloning of *psm*β operon	
Psmβ1Bam	CTTCAAATGGATCCTTTAAGGAGTGTTTTCAATGGAAGG
Psmβ2Mlu	CTGAGTGCATAACATACGCGTATGCTCACCCAGTTTATTTTAAAG

min at 37°C, and imaged using a Zeiss LSM700 confocal microscope. Total biovolume was calculated using Imaris software from three randomly chosen fields. This protocol was used for all biofilm CLSM analyses with the exception of the protocol used for the image shown in Fig. 1B, for which *S. aureus* (10^9 CFU/ml) was incubated in SF for 20 min, stained with 4 μM propidium iodide, and immediately imaged.

Measurement of PSMs. After butanol extraction of PSMs, PSM production was analyzed by reversed-phase high-pressure liquid chromatography/electrospray mass spectrometry as described previously (27).

Statistics. Statistical evaluation was performed using GraphPad Prism version 6.02, with *t* tests for the comparison of two and one-way ANOVA for the comparison of more than two groups. Multiple comparisons with one-way ANOVA were performed using Tukey's posttests.

RESULTS

Biofilms and free-floating aggregates form in synovial fluid isolated from patients. In the present study, we used an *ex vivo* ap-

TABLE 2 Strains and plasmids used in this study

Strain or plasmid	Description	Reference
Strains		
LAC	USA300, ST8, clinical CA-MRSA clone	
LAC Δ*agr*	*agr* mutant of strain LAC, obtained by phage transduction from strain RN6911	18
LAC Δ*psm*	Total *psm* deletion mutant; *psm*α and *psm*β operons are deleted; translation of *hld* is abolished by start codon mutation	21
LAC P2-*lux*	Strain LAC containing genome-integrated *luxABCDE* genes under the control of the *S. aureus* Agr P2 promoter	This study
LAC P3-*lux*	Strain LAC containing genome-integrated *luxABCDE* genes under the control of the *S. aureus* Agr P3 promoter	This study
LAC *psm*α-*lux*	Strain LAC containing genome-integrated *luxABCDE* genes under the control of the *S. aureus psm*α promoter	This study
LAC *psm*β-*lux*	Strain LAC containing genome-integrated *luxABCDE* genes under the control of the *S. aureus psm*β promoter	This study
Plasmids		
pTX$_{\Delta}$16	Control plasmid	18
pTX$_{\Delta}$*psm*α	Tet^{r}, *psm*α operon under constitutive control of the xylose promoter	18
pTX$_{\Delta}$*psm*β	Tet^{r}, *psm*β operon under constitutive control of the xylose promoter	This study
pTX$_{\Delta}$*hld*	Tet^{r}, *hld* gene under constitutive control of the xylose promoter	22
pTX$_{\Delta}$*agrA*	Tet^{r}, *agrA* gene under constitutive control of the xylose promoter	16

proach to study the mechanistic underpinnings of the formation of free-floating and surface-attached *S. aureus* agglomerates (biofilms) during prosthetic joint infection (PJI). We isolated synovial fluid (SF) from noninfected patients undergoing surgery, thus reproducing the environmental conditions the bacteria encounter when mounting a postoperative joint infection. All experiments were performed using strain LAC, representing pulsed-field type USA300, the predominant cause of PJI in the United States (19).

Even when SF was isolated from patients who had received high doses of prophylactic antibiotic, which leads to high concentrations of antibiotic in SF (28), biofilms formed on titanium disks over the course of 48 h (Fig. 1A), underscoring the notion that *S. aureus* PJIs are recalcitrant to antibiotic treatment due to the formation of biofilms (4, 28). Notably, extensive biofilm-like aggregates formed within minutes after incubation of the bacteria in SF and were characterized by the attachment of fibrous material (Fig. 1B and C).

Extreme agglomeration of *S. aureus* in SF is not due to increased expression of proteins interacting with host matrix molecules. We first analyzed expression of the factors determined in our previous transposon bank screen to be essential for aggregation in SF (4) and asked if increased expression of these factors causes the exceptional degree of agglomeration. These factors included mostly surface binding proteins, namely, the fibrinogen-binding proteins ClfA and ClfB and the fibronectin-binding proteins FnbA and FnbB (4). We have shown that the fibrinolytic protease plasmin can degrade the agglomerates, indicating that fibrin plays a major role among the host-derived factors that contribute to agglomerate formation (4). Furthermore, fibrin binding is considered more significant than binding to fibronectin, since fibrin concentration is higher in traumatized joints (9). The fibronectin-binding proteins showed increased expression in SF over serum and TSB (FnbA, 3.9 times higher than in TSB and 3.2 times higher than in serum; FnbB, 12.1 times higher than in TSB and 7.6 times higher than in serum) (Fig. 2). However, expression of the fibrinogen-binding proteins in SF was low in comparison, in particular in the case of ClfA (0.12 times higher than in TSB and 0.17 times higher than in serum) (Fig. 2). Furthermore, absolute expression values were by far highest for ClfA among the four surface binding proteins (highest mean Q_{gene}/Q_{gyrB} values [where Q_{gene} is the abundance of a given transcript and Q_{gyrB} is the abundance of the *gyrB* transcript] achieved: ClfA, 8.3; ClfB, 1.5; FnbA, 0.5; FnbB, 0.6), which is why the pronounced differences observed for this fibrinogen-binding protein matter most in relative terms (Fig. 2). Thus, while fibrinogen- and fibronectin-binding proteins are required as a basis of aggregate formation in SF, our results indicate that, taken together, differences in their expression do not appear to contribute considerably to the strong degree of aggregation behavior in SF.

Expression levels of the regulatory factors RsbU and TRAP also previously identified in our screen (4) were roughly equivalent in SF and serum, with a small increase over expression in TSB, indicating that these are also unlikely to be responsible for the strong aggregation phenotype (Fig. 2).

***S. aureus* shows low activity of Agr and low production of PSMs in SF.** As an alternative explanation, we evaluated whether low activity of the biofilm regulator Agr is responsible for the excessive formation of aggregates and biofilms in SF. To investigate this hypothesis, we constructed reporter gene fusion constructs. In these constructs, the *agr* P3 or P2 promoters were fused to the *lux* genes driving production of light-emitting luciferase. P3 drives expression of RNAIII, the intracellular regulator of most Agr targets (29), and P2 drives expression of the Agr proteins making up the Agr autoregulatory quorum-sensing circuit (30). Notably, all luciferase promoter fusions were cloned in the genome of strain LAC. In contrast to plasmid-based systems, which are often used for this purpose, genome insertion ensures that the obtained results accurately reflect natural expression and are not due to multiple, plasmid-introduced copies of the respective genes. During all stages of *in vitro* growth, Agr (P2 and P3) activity in human SF was extremely low, lower than in human serum and much lower than in TSB (Fig. 3A and B). This was verified using qRT-PCR with the *agrA* (controlled by the P2 promoter) and RNAIII (controlled by the P3 promoter) genes (Fig. 3C and D).

To analyze expression of the Agr-controlled PSMs in SF, we again used genome-integrated luciferase reporter gene constructs in strain LAC in addition to qRT-PCR measurements. The results confirmed our expectations, inasmuch as expression of the *psm*α and *psm*β loci was extremely low (Fig. 3E to G), as shown above for RNAIII (Fig. 3C), which also contains the *hld* gene encoding the δ-toxin. Furthermore, we measured PSM production on the

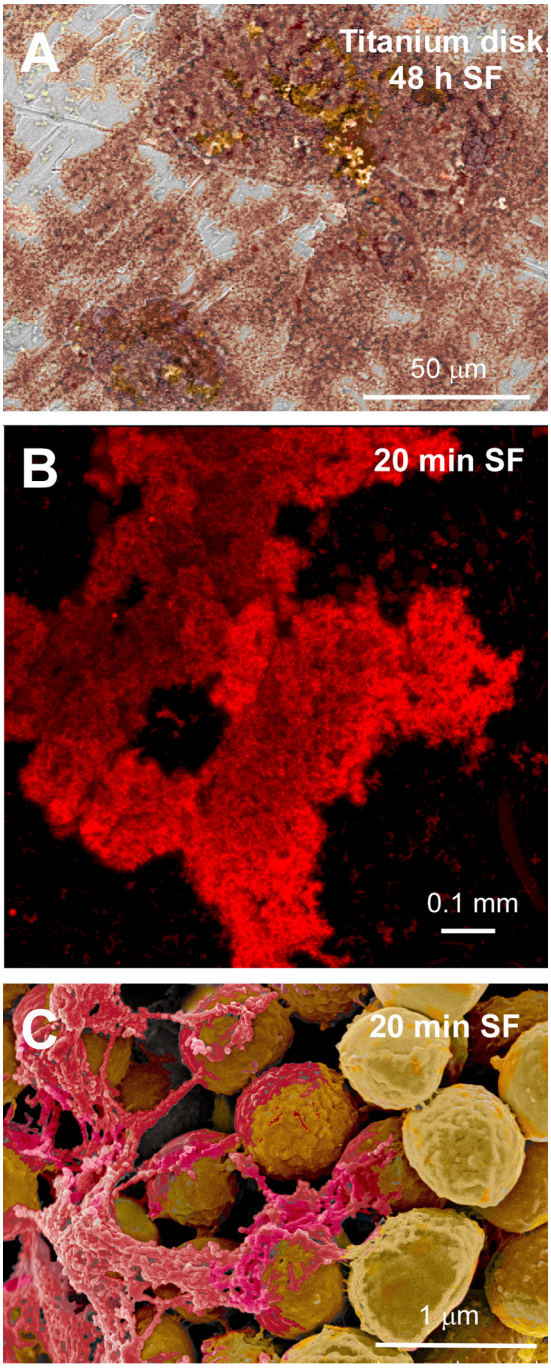

FIG 1 Synovial fluid promotes multicellular aggregation of *Staphylococcus aureus*. (A) Biofilm formation of *S. aureus* strain LAC (USA300) on a titanium disk incubated for 48 h in SF from a patient who had received 2 g of cefazolin. (B and C) Formation of free-floating aggregates of strain LAC inoculated from a preculture in TSB and incubated for 20 min in SF. Aggregates were imaged using CLSM (B) and SEM (A and C). Extracellular host-derived fibrous material is pseudocolored pink; *S. aureus* cells are yellow. (B) CLSM was performed with staining with propidium iodide, staining cells and matrix red.

protein level (Fig. 3H), which confirmed the results achieved on the transcriptional level. These results demonstrate extremely low production of all PSMs in SF and suggest that low PSM production is a major reason for the marked formation of aggregates in SF.

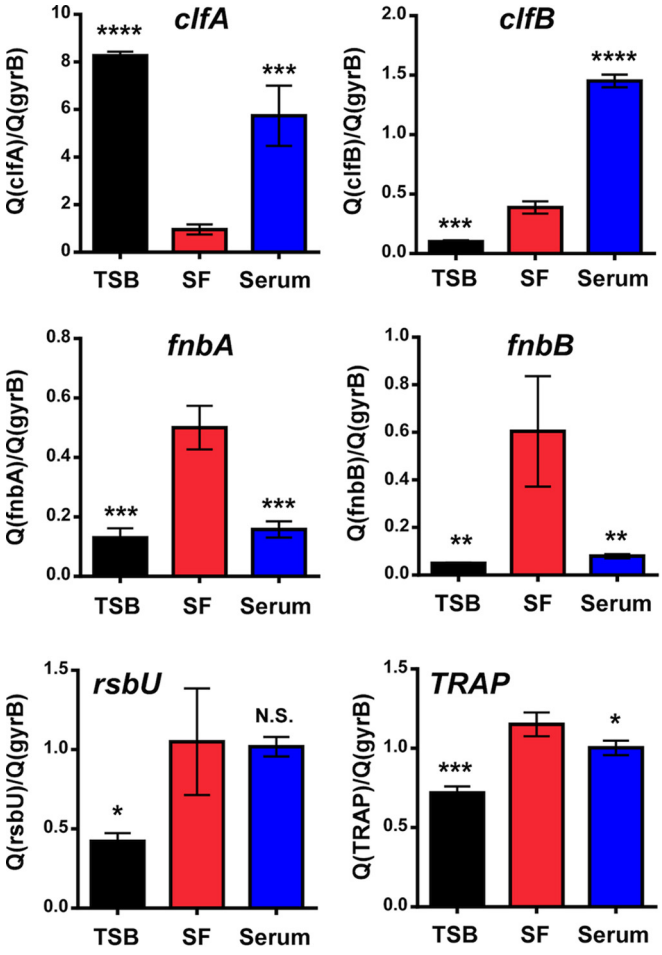

FIG 2 Expression of genes previously identified to be required for aggregation in SF (*clfA*, *clfB*, *fnbA*, *fnbB*, *trap*, and *rsbU*) in SF, TSB, and serum. The six genes previously identified by a transposon bank screen to be required for the aggregation behavior in SF were assayed by qRT-PCR for comparative expression in SF versus human serum and TSB. Samples were taken at 8 h of suspended growth. The experiments were performed in triplicate. Error bars show standard deviations (SD). *, $P < 0.05$; **, $P < 0.01$; ***, $P < 0.001$; ****, $P < 0.0001$.

Low production of the Agr-controlled phenol-soluble modulins is a major factor promoting bacterial aggregation and formation of biofilms in SF. To analyze whether the observed low activity of Agr in SF and low production of the biofilm-dispersing PSMs are responsible for the aggregative phenotype in SF, we determined the extent of bacterial agglomeration of wild-type and isogenic Δ*agr* and Δ*psm* mutants as visualized microscopically and using a Cellometer. In the Δ*psm* mutant, all *psm* genes have been removed or translation has been abolished (21). We found that all strains, notably including the wild-type strain, showed extensive agglomeration in SF, while in TSB, only Δ*agr* and Δ*psm* mutants produced agglomerates (Fig. 4). Furthermore, the extent of agglomeration in SF was not statistically different in the wild type and the Δ*agr* and Δ*psm* mutants. These results showed that low activity of Agr and suppression of the Agr-controlled PSMs cause exceptionally strong aggregate production in SF.

To provide further evidence for the role of PSMs and Agr in aggregation in SF and delineate the specific role of different PSM

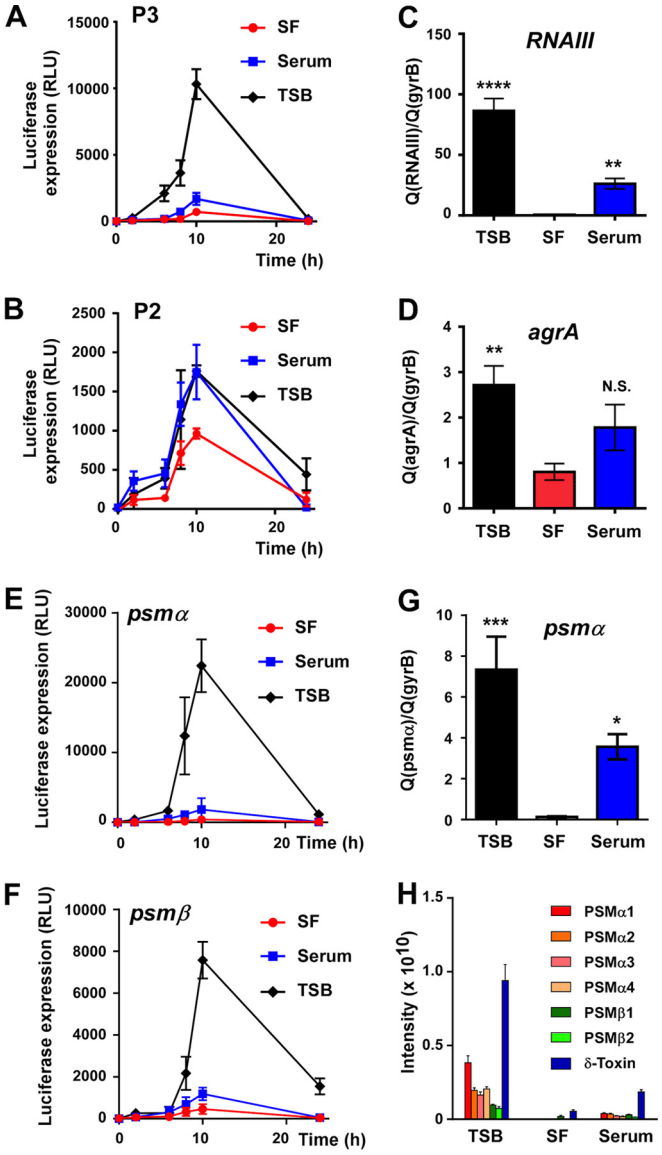

FIG 3 Agr activity and PSM production are low in synovial fluid. (A and B) Activity of the Agr P3 (A) and the Agr P2 promoter (B) measured during suspended growth in SF, human serum, or TSB, using genome-integrated, single-copy *luxABCDE* luciferase operon reporter fusion constructs. (C and D) Expression of RNAIII (C) and *agrA* (D) at 8 h of growth, measured by qRT-PCR. (E and F) Expression of *psm*α (E) and *psm*β (F) promoters during growth in SF, human serum, or TSB, using genome-integrated, single-copy *luxABCDE* luciferase operon reporter fusion constructs. (G) Expression of *psm*α operon by qRT-PCR, at 8 h of growth. (H) PSM production determined in culture filtrates after 8 h of growth. All experiments were performed in triplicate. Error bars show standard deviations (SD). *, $P < 0.05$; **, $P < 0.01$; ***, $P < 0.001$; ****, $P < 0.0001$.

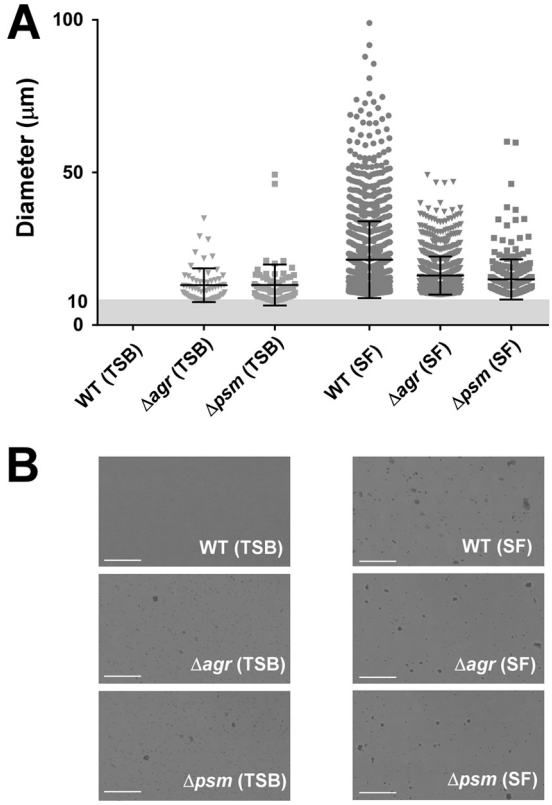

FIG 4 Aggregate size distribution after incubation of *S. aureus* under different conditions. (A) Size distribution of aggregates, measured by a Cellometer, after 20 min incubation in the respective fluids (SF or TSB) of LAC wild-type (WT), isogenic Δ*agr* deletion, or total Δ*psm* deletion strains. Aggregates between 10 and 100 μm were determined; larger aggregates cannot be measured by this method. (B) Corresponding representative microscopic pictures. Note the absence of clusters in the TSB wild-type sample in both panels. Scale bars, 50 μm.

types, we transformed the LAC wild-type strain with plasmids carrying the *psm*α, *psm*β, *hld* (encoding δ-toxin), or *agrA* genes/operons under the control of a constitutively active promoter. In these constructs, low expression of those genes in SF is thus overcome by constitutive expression. We first analyzed the formation of macroscopic clusters during 24-h growth in microtiter plates. In SF, the LAC wild-type strain formed a large cluster, in accordance with our previous results (4); this was not the case in serum or TSB (Fig. 5). Importantly, no cluster formation was visible when the strains expressing *psm*α, *psm*β, or *hld* genes/operons were incubated in SF. Similarly, no cluster formation was detected when *agrA*, which controls expression of all of these genes, was expressed (16). Furthermore, the Δ*psm* mutant, devoid of PSM production, showed large cluster formation in SF, similar to that observed with the wild-type and Δ*agr* strain.

We next analyzed biofilm formation of the constitutive-expression constructs by confocal laser scanning microscopy (CLSM) with an analysis of total biovolume. Similar to the results obtained for macroscopic cluster formation, biofilm formation by the constructs expressing *psm*α, *psm*β, *hld*, or *agrA* was significantly less pronounced than that by the wild-type strain (Fig. 6). Together, these results identify the lack of PSM production as the main cause for the extensive biofilm and aggregate formation in SF and show that all PSM types have the capacity to disrupt aggregates.

PSMs work by dispersing biofilm matrix molecules such as PIA. The surfactant characteristics of PSMs suggest that these molecules function during biofilm development by disrupting the interaction of biofilm matrix molecules with each other and the bacterial cell surface (31). However, this has not yet been examined experimentally. PIA is considered a major biofilm matrix

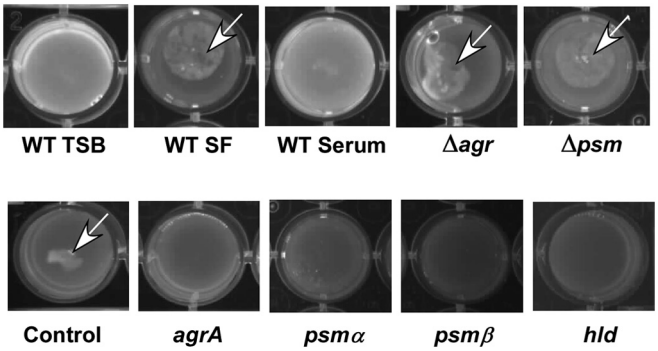

FIG 5 PSM expression abolishes the formation of macroscopic cell clusters in SF. The LAC wild-type strain (WT) was inoculated into 200 μl SF, human serum, or TSB at 10^4 CFU and incubated under static conditions for 18 h. In addition, the LAC Δ*agr* and Δ*psm* strains and derivatives of the LAC wild-type strain containing either plasmids (pTX_Δ) for constitutive expression of *agrA*, *psm*α, *psm*β, or *hld* genes or a control plasmid ($pTX_\Delta16$) were inoculated and grown under the same conditions in SF. Plasmid-containing strains received 12.5 μg/ml tetracycline for plasmid maintenance. Afterwards, cell clusters were visualized by staining with ethidium bromide. Note that large clusters formed only in the WT (when grown in SF) and SF-grown Δ*agr*, Δ*psm*, and plasmid control samples (arrows), whereas expression of any of the *psm* loci or the PSM regulator *agrA* resulted in abolishment of cluster formation.

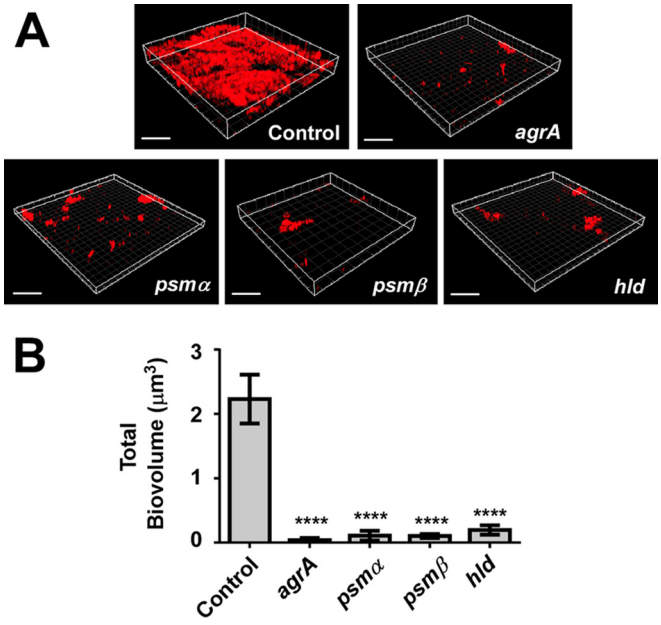

FIG 6 PSM expression abolishes biofilm formation in SF. (A) Derivatives of the LAC wild-type strain containing plasmids (pTX_Δ) for constitutive expression of *agrA*, *psm*α, *psm*β, or *hld* genes or a control plasmid ($pTX_{\Delta16}$) were assayed for biofilm formation in SF under static conditions (24-h growth). Plasmid-containing strains received 12.5 μg/ml tetracycline for plasmid maintenance. Biofilms were stained with propidium iodide for CLSM. (B) The total biovolume was calculated using Imaris software using 3 randomly chosen image fields. Error bars show standard deviations (SD). ****, $P < 0.0001$.

component in staphylococci (6). We showed previously that strain LAC produces a large amount of surface-located PIA when grown in SF (4). Transcription of the *ica* PIA biosynthesis operon (as determined by qRT-PCR of the *icaA* gene) was not increased in SF (Fig. 7A). However, immunological assessment using PIA-specific antibodies revealed that (i) PIA retention on the bacterial surface was significantly higher in SF than TSB and serum (Fig. 7B) and (ii) PIA was released from the bacterial surface in a PSM-dependent manner (Fig. 7C). The latter was demonstrated by the fact that surface PIA levels were similarly high in the isogenic Δ*psm* mutant when it was grown in either TSB or SF and in the wild-type strain grown in SF (conditions without or with very low PSM production) but significantly higher than PIA surface levels in the wild-type strain grown in TSB (under which condition PSMs are produced) (Fig. 7C). These results suggest that PIA matrix molecules are abundant on the bacterial surface in the absence of PSMs, indicating that PSMs cause separation of the PIA matrix molecules from the bacterial surface.

To provide further evidence supporting that mechanism, we compared cluster formation of the wild-type and Δ*psm* mutant strains using scanning electron microscopy (SEM). This was done in TSB, because (i) there is no host-derived fibrous material overshadowing bacterial exopolymers during growth in TSB and (ii) we have shown here that there is virtually no PSM production in SF. SEM showed only single cells and no cluster formation of the wild-type strain (in accordance with the results shown in Fig. 4). In contrast, the Δ*psm* mutant formed clusters, which had fibrous material on their surface (Fig. 7D), which—in the absence of host material such as fibrin—are strongly indicative of the deposition of bacterial biofilm matrix molecules, such as PIA, but also likely includes other biofilm matrix components, such as teichoic acids, extracellular DNA, and biofilm matrix proteins. Thus, these findings further confirmed that PSMs interfere with the deposition of matrix molecules on the bacterial surface.

DISCUSSION

In our previous study, we discovered that *S. aureus* proteins that connect the bacteria to the human matrix proteins fibrin and fibronectin are prerequisites for the formation of biofilms and biofilm-like aggregates during joint infections (4). In the present study, we asked which factors are responsible for the excessively strong degree of aggregate and biofilm formation in SF, which is the basis for the notorious recalcitrance of such infections to antibiotic treatment (28). We identified the low activity of Agr and consequentially low production of PSMs as major factors contributing to that phenotype. Our results support a two-step model of aggregate formation during joint infection which includes (i) bacterial attachment to fibrin and fibronectin via ClfA, ClfB, FnbA, and FnbB and (ii) extensive agglomeration of cells and bacterial matrix molecules, owing to the absence of the surfactant-like, separating effect of the Agr-controlled PSMs. It appears surprising at first glance that there is low activity of the quorum-sensing regulator Agr in cellular aggregates, despite such aggregates representing a high-cell-density situation. However, we and others have observed overall low activity of Agr activity in *in vitro* staphylococcal biofilms (11, 12, 32). Furthermore, there has been considerable doubt about a direct correlation of cell density and the activity of quorum-sensing systems (33). Whether the low activity of Agr in SF is due to specific factors that are present in SF, such as hyaluronic acid (34, 35), or the overall chemical composition of SF (35) awaits further investigation. One specific possibility that remains to be explored is whether the increased concentration of serum proteins in traumatized SF (36) contributes to a quorum-quenching effect due to sequestration of the Agr pheromone, as described for apolipoprotein B (37).

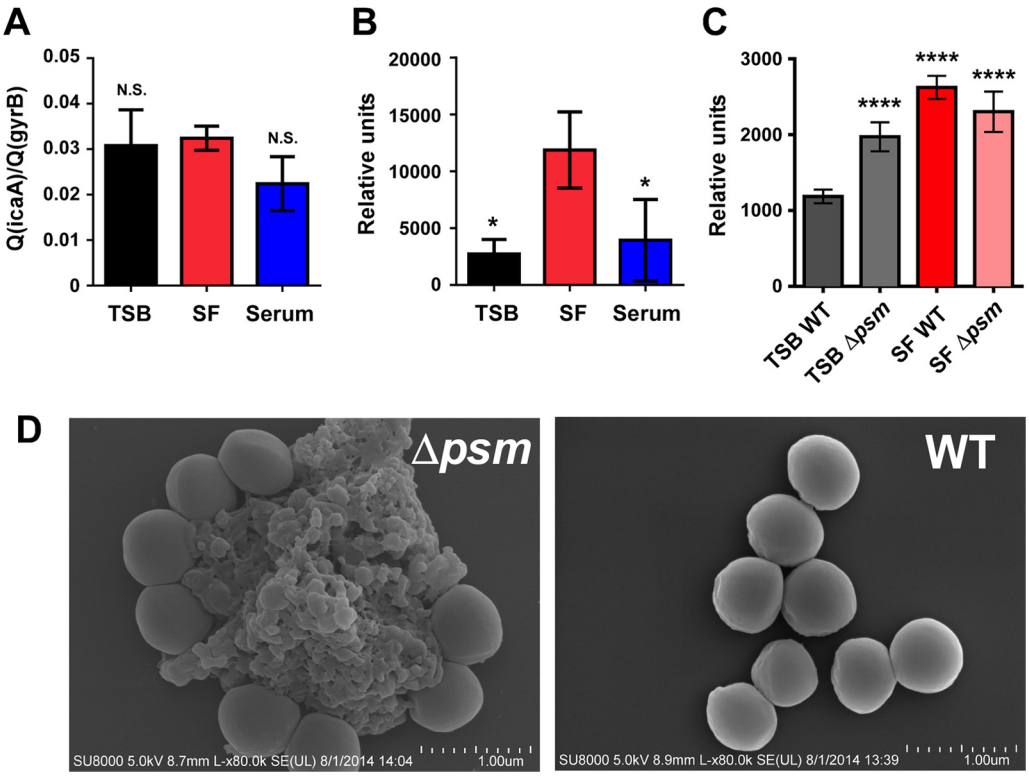

FIG 7 Growth in SF leads to increased retention of the biofilm exopolysaccharide PIA on cells. (A) Expression of PIA biosynthetic operon (measured by qRT-PCR of the *icaA* gene) at 8 h of growth under different conditions. (B and C) Cell-bound PIA after 12 h of growth, measured using detection by anti-PIA antiserum in immune dot blots followed by densitometry. Error bars show standard deviations (SD). *, $P < 0.05$; ****, $P < 0.0001$ (1-way ANOVA versus the SF value [B] and versus the WT SF value [C]). (D) Wild-type LAC (WT) and the PSM-free isogenic Δ*psm* strain were grown for 8 h in TSB, and bacterial cells were assayed by SEM. Cell clusters were not found in the wild-type strain but were found in high numbers in the Δ*psm* strain (also compare the results shown in Fig. 3, obtained using a Cellometer).

The significance of our results extends beyond joint infection. For the first time, we provide evidence in a system closely resembling *in vivo* conditions, and this evidence underscores a key role of PSM production in defining the extent of *S. aureus* biofilms. Specifically, we demonstrate that low PSM production causes strongly increased biofilm formation. Furthermore, we show that absence of PSMs leads to increased formation of floating aggregates, which was shown previously only for surface-attached biofilms (13, 15). Moreover, our results provide previously unavailable evidence for the mechanism by which PSMs disperse biofilms, inasmuch as we demonstrate PSM-dependent release of PIA from the bacterial surface.

Our results are of particular interest given that *in vitro* studies have led to two different models of how PSM production impacts *S. aureus* biofilm development. Our previous studies, performed using TSB, indicated that absence of PSMs leads to more extensive and compact biofilm formation, owing to a lack of PSM-mediated biofilm structuring and dispersal (13). In contrast, using a different growth medium, Schwartz et al. observed that PSMs form amyloid-like fibrils that promote (rather than decrease) biofilm formation *in vitro* (38). In our present study, we demonstrate that under conditions emulating the *in vivo* situation present during a biofilm-associated infection, absence of PSMs leads to extensive formation of biofilms, while the amyloid model of Schwartz et al. would have predicted that in the absence of PSMs, biofilms would be less pronounced. In accordance with our previous *in vivo* results (13), our present findings further suggest that the role of PSM amyloid fibrils in biofilm development applies only to a very specific *in vitro* setup.

Our results further support the notion that differences in Agr activity are associated with different types of staphylococcal infection and demonstrate the crucial role that PSMs play in that association. Mutants that are dysfunctional in Agr have been found more frequently in chronic, biofilm-associated infections (14, 39) and in cases of *S. aureus* bacteremia (40). In contrast, a functional Agr system and high production of Agr-regulated toxins, such as PSMs and alpha-toxin, are associated with acute forms of *S. aureus* infection, such as acute skin and lung infections (18, 41, 42), and osteomyelitis (43). Since there is continual developing of drugs targeting the Agr system (44), we caution that the use of Agr-blocking therapeutics should be limited to certain infection types and would be counterproductive in others.

In conclusion, the findings from our study indicate that the exceptional recalcitrance of staphylococcal PJI to antibiotic treatment (28) is due to the specific environment in joints that suppresses Agr and production of biofilm-dispersing PSMs, which together with the interaction with host-derived fibrin leads to the formation of extensive bacterial agglomerates. These results further our understanding about the role Agr and PSMs play in defining biofilm-associated *S. aureus* disease, which could lead to the development of antibiofilm therapeutic strategies against PJI. Our findings suggest that therapeutic strategies against staphylococcal

PJI should target the host-derived and bacterial factors that contribute to agglomerate formation, such as fibrin and bacterial biofilm matrix molecules, including PIA.

ACKNOWLEDGMENTS

This study was supported by the Intramural Research Program of the National Institute of Allergy and Infectious Diseases (NIAID), U.S. National Institutes of Health (NIH) (ZIA AI000904-13, to M.O.). This study was also supported by NIH grants HD06153 and DE019901 to N.J.H., and S.S.D. was supported by a T32 NIH training grant (T32-AR-052273).

We thank Chia Lee and Kevin Francis for providing plasmids and Javad Parvizi for collecting synovial fluid. We also thank Irving M. Shapiro for thoughtful discussions.

REFERENCES

1. **Shirtliff ME, Mader JT.** 2002. Acute septic arthritis. Clin Microbiol Rev **15:**527–544. http://dx.doi.org/10.1128/CMR.15.4.527-544.2002.
2. **Kurtz SM, Lau E, Watson H, Schmier JK, Parvizi J.** 2012. Economic burden of periprosthetic joint infection in the United States. J Arthroplasty **27:**61–65.e1. http://dx.doi.org/10.1016/j.arth.2012.02.022.
3. **Zimmerli W, Trampuz A, Ochsner PE.** 2004. Prosthetic-joint infections. N Engl J Med **351:**1645–1654. http://dx.doi.org/10.1056/NEJMra040181.
4. **Dastgheyb S, Parvizi J, Shapiro IM, Hickok NJ, Otto M.** 2015. Effect of biofilms on recalcitrance of staphylococcal joint infection to antibiotic treatment. J Infect Dis **211:**641–650. http://dx.doi.org/10.1093/infdis/jiu514.
5. **Donlan RM.** 2001. Biofilms and device-associated infections. Emerg Infect Dis **7:**277–281. http://dx.doi.org/10.3201/eid0702.010226.
6. **Otto M.** 2008. Staphylococcal biofilms. Curr Top Microbiol Immunol **322:**207–228.
7. **Cramton SE, Gerke C, Schnell NF, Nichols WW, Gotz F.** 1999. The intercellular adhesion (*ica*) locus is present in *Staphylococcus aureus* and is required for biofilm formation. Infect Immun **67:**5427–5433.
8. **Mack D, Fischer W, Krokotsch A, Leopold K, Hartmann R, Egge H, Laufs R.** 1996. The intercellular adhesin involved in biofilm accumulation of *Staphylococcus epidermidis* is a linear beta-1,6-linked glucosaminoglycan: purification and structural analysis. J Bacteriol **178:**175–183.
9. **Lack CH.** 1959. Chondrolysis in arthritis. J Bone Joint Surg Br **41–B:**384–387.
10. **Kornblum J, Kreiswirth B, Projan SJ, Ross H, Novick RP.** 1990. agr; a polycistronic locus regulating exoprotein synthesis in *Staphylococcus aureus*, p 373–402. *In* Novick RP (ed), Molecular biology of the staphylococci. VCH Publishers, New York, NY.
11. **Vuong C, Saenz HL, Gotz F, Otto M.** 2000. Impact of the agr quorum-sensing system on adherence to polystyrene in *Staphylococcus aureus*. J Infect Dis **182:**1688–1693. http://dx.doi.org/10.1086/317606.
12. **Yarwood JM, Bartels DJ, Volper EM, Greenberg EP.** 2004. Quorum sensing in *Staphylococcus aureus* biofilms. J Bacteriol **186:**1838–1850. http://dx.doi.org/10.1128/JB.186.6.1838-1850.2004.
13. **Periasamy S, Joo HS, Duong AC, Bach TH, Tan VY, Chatterjee SS, Cheung GY, Otto M.** 2012. How *Staphylococcus aureus* biofilms develop their characteristic structure. Proc Natl Acad Sci U S A **109:**1281–1286. http://dx.doi.org/10.1073/pnas.1115006109.
14. **Vuong C, Kocianova S, Yao Y, Carmody AB, Otto M.** 2004. Increased colonization of indwelling medical devices by quorum-sensing mutants of *Staphylococcus epidermidis* in vivo. J Infect Dis **190:**1498–1505. http://dx.doi.org/10.1086/424487.
15. **Wang R, Khan BA, Cheung GY, Bach TH, Jameson-Lee M, Kong KF, Queck SY, Otto M.** 2011. *Staphylococcus epidermidis* surfactant peptides promote biofilm maturation and dissemination of biofilm-associated infection in mice. J Clin Invest **121:**238–248. http://dx.doi.org/10.1172/JCI42520.
16. **Queck SY, Jameson-Lee M, Villaruz AE, Bach TH, Khan BA, Sturdevant DE, Ricklefs SM, Li M, Otto M.** 2008. RNAIII-independent target gene control by the agr quorum-sensing system: insight into the evolution of virulence regulation in *Staphylococcus aureus*. Mol Cell **32:**150–158. http://dx.doi.org/10.1016/j.molcel.2008.08.005.
17. **Peschel A, Otto M.** 2013. Phenol-soluble modulins and staphylococcal infection. Nat Rev Microbiol **11:**667–673. http://dx.doi.org/10.1038/nrmicro3110.
18. **Wang R, Braughton KR, Kretschmer D, Bach TH, Queck SY, Li M, Kennedy AD, Dorward DW, Klebanoff SJ, Peschel A, DeLeo FR, Otto M.** 2007. Identification of novel cytolytic peptides as key virulence determinants for community-associated MRSA. Nat Med **13:**1510–1514. http://dx.doi.org/10.1038/nm1656.
19. **Kourbatova EV, Halvosa JS, King MD, Ray SM, White N, Blumberg HM.** 2005. Emergence of community-associated methicillin-resistant *Staphylococcus aureus* USA 300 clone as a cause of health care-associated infections among patients with prosthetic joint infections. Am J Infect Control **33:**385–391. http://dx.doi.org/10.1016/j.ajic.2005.06.006.
20. **DeLeo FR, Otto M, Kreiswirth BN, Chambers HF.** 2010. Community-associated meticillin-resistant *Staphylococcus aureus*. Lancet **375:**1557–1568. http://dx.doi.org/10.1016/S0140-6736(09)61999-1.
21. **Joo HS, Cheung GY, Otto M.** 2011. Antimicrobial activity of community-associated methicillin-resistant *Staphylococcus aureus* is caused by phenol-soluble modulin derivatives. J Biol Chem **286:**8933–8940. http://dx.doi.org/10.1074/jbc.M111.221382.
22. **Nakamura Y, Oscherwitz J, Cease KB, Chan SM, Munoz-Planillo R, Hasegawa M, Villaruz AE, Cheung GY, McGavin MJ, Travers JB, Otto M, Inohara N, Nunez G.** 2013. Staphylococcus delta-toxin induces allergic skin disease by activating mast cells. Nature **503:**397–401. http://dx.doi.org/10.1038/nature12655.
23. **Li M, Cha DJ, Lai Y, Villaruz AE, Sturdevant DE, Otto M.** 2007. The antimicrobial peptide-sensing system aps of *Staphylococcus aureus*. Mol Microbiol **66:**1136–1147. http://dx.doi.org/10.1111/j.1365-2958.2007.05986.x.
24. **Francis KP, Joh D, Bellinger-Kawahara C, Hawkinson MJ, Purchio TF, Contag PR.** 2000. Monitoring bioluminescent *Staphylococcus aureus* infections in living mice using a novel *luxABCDE* construct. Infect Immun **68:**3594–3600. http://dx.doi.org/10.1128/IAI.68.6.3594-3600.2000.
25. **Luong TT, Lee CY.** 2007. Improved single-copy integration vectors for *Staphylococcus aureus*. J Microbiol Methods **70:**186–190. http://dx.doi.org/10.1016/j.mimet.2007.04.007.
26. **Cramton SE, Gerke C, Gotz F.** 2001. In vitro methods to study staphylococcal biofilm formation. Methods Enzymol **336:**239–255. http://dx.doi.org/10.1016/S0076-6879(01)36593-X.
27. **Joo HS, Otto M.** 2014. The isolation and analysis of phenol-soluble modulins of *Staphylococcus epidermidis*. Methods Mol Biol **1106:**93–100. http://dx.doi.org/10.1007/978-1-62703-736-5_7.
28. **Dastgheyb S, Hammoud S, Ketonis C, Liu AY, Fitzgerald K, Parvizi J, Purtill J, Ciccotti M, Shapiro IM, Otto M, Hickok NJ.** 2015. Staphylococcal persistence due to biofilm formation in synovial fluid containing prophylactic cefazolin. Antimicrob Agents Chemother **59:**2122–2128. http://dx.doi.org/10.1128/AAC.04579-14.
29. **Novick RP, Ross HF, Projan SJ, Kornblum J, Kreiswirth B, Moghazeh S.** 1993. Synthesis of staphylococcal virulence factors is controlled by a regulatory RNA molecule. EMBO J **12:**3967–3975.
30. **Novick RP, Projan SJ, Kornblum J, Ross HF, Ji G, Kreiswirth B, Vandenesch F, Moghazeh S.** 1995. The agr P2 operon: an autocatalytic sensory transduction system in *Staphylococcus aureus*. Mol Gen Genet **248:**446–458. http://dx.doi.org/10.1007/BF02191645.
31. **Hall PR, Elmore BO, Spang CH, Alexander SM, Manifold-Wheeler BC, Castleman MJ, Daly SM, Peterson MM, Sully EK, Femling JK, Otto M, Horswill AR, Timmins GS, Gresham HD.** 2013. Nox2 modification of LDL is essential for optimal apolipoprotein B-mediated control of agr type III *Staphylococcus aureus* quorum-sensing. PLoS Pathog **9:**e1003166. http://dx.doi.org/10.1371/journal.ppat.1003166.
32. **Vuong C, Gerke C, Somerville GA, Fischer ER, Otto M.** 2003. Quorum-sensing control of biofilm factors in *Staphylococcus epidermidis*. J Infect Dis **188:**706–718. http://dx.doi.org/10.1086/377239.
33. **Redfield RJ.** 2002. Is quorum sensing a side effect of diffusion sensing? Trends Microbiol **10:**365–370. http://dx.doi.org/10.1016/S0966-842X(02)02400-9.
34. **Blau S, Janis R, Hamerman D, Sandson J.** 1965. Cellular origin of hyaluronateprotein in human synovial membrane. Science **150:**353–355. http://dx.doi.org/10.1126/science.150.3694.353.
35. **Ropes MW, Rossmeisl EC, Bauer W.** 1940. The origin and nature of normal human synovial fluid. J Clin Invest **19:**795–799. http://dx.doi.org/10.1172/JCI101182.
36. **Kim WJ, Ahn YS, Kim SJ, Jahng JS, Hong SS.** 1976. Study on the fractionation of synovial fluid protein. Yonsei Med J **17:**109–114. http://dx.doi.org/10.3349/ymj.1976.17.2.109.
37. **Peterson MM, Mack JL, Hall PR, Alsup AA, Alexander SM, Sully EK, Sawires YS, Cheung AL, Otto M, Gresham HD.** 2008. Apolipoprotein

B is an innate barrier against invasive *Staphylococcus aureus* infection. Cell Host Microbe **4:**555–566. http://dx.doi.org/10.1016/j.chom.2008.10.001.

38. **Schwartz K, Syed AK, Stephenson RE, Rickard AH, Boles BR.** 2012. Functional amyloids composed of phenol soluble modulins stabilize *Staphylococcus aureus* biofilms. PLoS Pathog **8:**e1002744. http://dx.doi.org/10.1371/journal.ppat.1002744.
39. **Traber KE, Lee E, Benson S, Corrigan R, Cantera M, Shopsin B, Novick RP.** 2008. agr function in clinical *Staphylococcus aureus* isolates. Microbiology **154:**2265–2274. http://dx.doi.org/10.1099/mic.0.2007/011874-0.
40. **Fowler VG, Jr, Sakoulas G, McIntyre LM, Meka VG, Arbeit RD, Cabell CH, Stryjewski ME, Eliopoulos GM, Reller LB, Corey GR, Jones T, Lucindo N, Yeaman MR, Bayer AS.** 2004. Persistent bacteremia due to methicillin-resistant *Staphylococcus aureus* infection is associated with agr dysfunction and low-level in vitro resistance to thrombin-induced platelet microbicidal protein. J Infect Dis **190:**1140–1149. http://dx.doi.org/10.1086/423145.
41. **Bubeck Wardenburg J, Bae T, Otto M, DeLeo FR, Schneewind O.** 2007. Poring over pores: alpha-hemolysin and Panton-Valentine leukocidin in *Staphylococcus aureus* pneumonia. Nat Med **13:**1405–1406. http://dx.doi.org/10.1038/nm1207-1405.
42. **Cheung GY, Wang R, Khan BA, Sturdevant DE, Otto M.** 2011. Role of the accessory gene regulator agr in community-associated methicillin-resistant *Staphylococcus aureus* pathogenesis. Infect Immun **79:**1927–1935. http://dx.doi.org/10.1128/IAI.00046-11.
43. **Cassat JE, Hammer ND, Campbell JP, Benson MA, Perrien DS, Mrak LN, Smeltzer MS, Torres VJ, Skaar EP.** 2013. A secreted bacterial protease tailors the *Staphylococcus aureus* virulence repertoire to modulate bone remodeling during osteomyelitis. Cell Host Microbe **13:**759–772. http://dx.doi.org/10.1016/j.chom.2013.05.003.
44. **Khan BA, Yeh AJ, Cheung GY, Otto M.** 2015. Investigational therapies targeting quorum-sensing for the treatment of *Staphylococcus aureus* infections. Expert Opin Invest Drugs **24:**689–704. http://dx.doi.org/10.1517/13543784.2015.1019062.